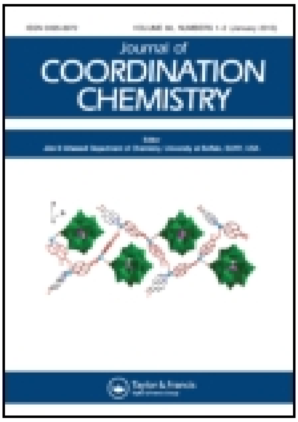

Journal of Coordination Chemistry
Publication details, including instructions for authors and subscription information:
http://www.tandfonline.com/loi/gcoo20

Synthesis, characterization, EPR, electrochemical, and in situ spectroelectrochemical studies of salen-type oxovanadium(IV) and copper(II) complexes derived from 3,4-diaminobenzophenone

Ayşe Erçağ [a] , Musa Şahin [a] , Atif Koca [b] & Esat Bozkurt [c]
[a] Engineering Faculty, Department of Chemistry , Istanbul University , Istanbul , Turkey
[b] Engineering Faculty, Department of Chemical Engineering , Marmara University , Istanbul , Turkey
[c] Faculty of Arts and Sciences, Department of Physics , Ondokuz Mayis University , Samsun , Turkey

Accepted author version posted online: 22 Mar 2013.Published online: 29 Apr 2013.

To cite this article: Ayşe Erçağ , Musa Şahin , Atif Koca & Esat Bozkurt (2013) Synthesis, characterization, EPR, electrochemical, and in situ spectroelectrochemical studies of salen-type oxovanadium(IV) and copper(II) complexes derived from 3,4-diaminobenzophenone, Journal of Coordination Chemistry, 66:9, 1635-1649, DOI: 10.1080/00958972.2013.787530

To link to this article: http://dx.doi.org/10.1080/00958972.2013.787530

Journal of Coordination Chemistry, 2013
Vol. 66, No. 9, 1635–1649, http://dx.doi.org/10.1080/00958972.2013.787530

Taylor & Francis
Taylor & Francis Group

Synthesis, characterization, EPR, electrochemical, and *in situ* spectroelectrochemical studies of salen-type oxovanadium(IV) and copper(II) complexes derived from 3,4-diaminobenzophenone

AYŞE ERÇAĞ*†, MUSA ŞAHIN†, ATIF KOCA‡ and ESAT BOZKURT§

†Engineering Faculty, Department of Chemistry, Istanbul University, Istanbul, Turkey
‡Engineering Faculty, Department of Chemical Engineering, Marmara University, Istanbul, Turkey
§Faculty of Arts and Sciences, Department of Physics, Ondokuz Mayis University, Samsun, Turkey

(*Received 4 December 2012; in final form 22 January 2013*)

A new half unit and some new symmetrical or asymmetrical VO(IV) and Cu(II) complexes of tetradentate ONNO Schiff base ligands were synthesized. The probable structures of the complexes have been proposed on the basis of elemental analyses and spectral (IR, UV–Vis, electron paramagnetic resonance, ESI-MS) data. VO(IV) and Cu(II) complexes exhibit square pyramidal and square-planar geometries, respectively. The complexes are non-electrolytes in dimethylformamide (DMF) and dimethylsulfoxide. Electrochemical behaviors of the complexes were studied using cyclic voltammetry and square wave voltammetry. Half-wave potentials ($E_{1/2}$) are significantly influenced by the central metal and slightly influenced by the nature of substituents on salen. While VO (IV) complexes give VO^{IV}/VO^{V} redox couples and a ligand-based reduction process, Cu(II) complexes give only a ligand-based reduction. *In situ* spectroelectrochemical studies were employed to determine the spectra of electrogenerated species of the complexes and to assign the redox processes. The *g*-values were calculated for all these complexes in polycrystalline state at 298 K and in frozen DMF (113 K). The evaluated metal–ligand bonding parameters showed strong in-plane σ-bonding for some Cu(II) complexes.

Keywords: Schiff base; Metal complexes; 3,4-Diaminobenzophenone; Electrochemistry; Spectroelectrochemistry; EPR

1. Introduction

Schiff bases bind metal ions leading to complexes with interesting properties. Salen complexes of transition metals have been used in solution as biomimetic catalysts for oxygen atom transfer and as catalysts for enantioselective epoxidation, aziridinations, mediating organic redox reactions, and other oxidative processes [1–3].

Asymmetrical Schiff bases offer advantages over their symmetrical counterparts in elucidation of composition and geometry of the metal ion binding sites in metallo-proteins and enzymes, and selectivity of natural systems with synthetic materials [4].

---

*Corresponding author. Email: ercaga@istanbul.edu.tr

Several vanadium complexes of tetradentate salen-type Schiff bases have been proposed for treatment of obesity and hypertension [5, 6]. A major advance in the use of vanadium has been the development of organic vanadium complexes [7], and the increase in interest in the bio-inorganic chemistry of vanadium has been documented by two monographs [8, 9].

Vanadium and copper complexes are model compounds for clarification of biochemical processes [10, 11]. We chose salen for this investigation because its ligand framework is similar to porphyrins. Porphyrin and Schiff base ligands are capable of supporting metals in a variety of oxidation states [12].

Vanadyl complexes of Schiff bases have two attractive properties. One is the d^1 configuration which is important to biological systems because it allows electron paramagnetic resonance (EPR) to probe ligand bio-environments [13–16]. The other property is catalytic reactivity toward organic substrates, in particular oxidation of organic substrates such as alkenes and sulfides [17]. When chiral Schiff bases are used as ligands, vanadyl complexes can effectively catalyze asymmetric oxidation of sulfides [18–20], disulfides [21], and dithioacetals [22].

Electrochemical methods provide valuable information regarding catalytic processes since catalytic conversions are frequently accompanied by change in structure of the complex and oxidation state of the metal; however, electrochemical approaches have not been fully explored. Knowledge of the electronic and steric effects that control redox chemistry of these metal complexes may prove critical in the design of new catalysts. Vanadium can be found from +3 to +5 and can be converted by one-electron redox reactions [23]. The oxidation–reduction and the coordination chemistry of vanadium explain most of its biochemistry [24].

Copper is found in all living organisms and is a crucial trace element in redox chemistry, growth, and development. It is important for the function of several enzymes and proteins involved in energy metabolism, respiration, and DNA synthesis, notably cytochrome oxidase, superoxide dismutase, ascorbate oxidase, and tyrosinase. The major functions of copper-biological molecules involve oxidation–reduction reactions in which they react directly with molecular oxygen to produce free radicals.

The stereospecific transformation of Cu(II) complexes as groove binder and intercalative mode of binding of the complex to the DNA was studied by electron spin resonance [25].

Here, we report the synthesis and characterization of a new half unit and some oxovanadium(IV) and copper(II) complexes of unsymmetrical (**1–6**) and symmetrical (**7–12**) tetradentate Schiff bases derived from 3,4-diaminobenzophenone (DAB) or the half unit. Spectral, magnetic properties, and comparative electrochemical studies of the complexes were studied.

Salen complexes have been used as electrocatalysts [26–28] and sensors [29–31]. For example, vanadyl salen complexes were used as electrocatalysts for four-electron reduction of molecular oxygen [32, 33]. These applications of salen complexes depend on the redox properties of the relevant complexes. Thus, to determine the possible technological application of the complexes studied here, we investigated the electrochemical properties of the complexes. *In situ* spectroelectrochemical studies were also employed for the first time to determine the spectra of the electrogenerated species.

We have also determined both structural and magnetic properties of symmetrical–asymmetrical salen-type oxovanadium(IV) and copper(II) complexes derived from DAB. A transition metal ion can be considered as a probe and used to determine the symmetry of the complexes in host lattices by EPR [34–37].

2. Experimental

2.1. *Reagents*

All chemicals were analytical grade. Solvents (ethanol, dichloromethane [DCM], methanol, diethyl ether, dimethylformamide [DMF] and dimethylsulfoxide [DMSO]) were reagent grade and used without purification. Salicylaldehyde was distilled before use.

2.2. *Physical measurements*

Elemental analyses were determined on a Thermo Finnigan Flash EA 1112 Series Elemental Analyser. FT-IR spectra were recorded from 4000 to 400 cm^{-1} with a Mattson 1000 FTIR spectrometer using KBr pellets. ^{1}H-NMR spectra were recorded on a Bruker AVANCE 500 MHz spectrometer, relative to $SiMe_4$ (tetramethylsilane) as an internal standard, using $CDCl_3$. Molar conductance measurements of the complexes (10^{-3} M) in DMSO were carried out with a WPA conductivity meter. Electronic spectra were recorded at room temperature on a ATI-Unicam UV2 spectrophotometer in DMSO. Mass spectra were recorded on a Thermo Finnigan LCQ Advantage Max LC/MS/MS.

Electrochemical and spectroelectrochemical measurements were carried out with a Gamry Reference 600 potentiostat/galvanostat utilizing a three-electrode configuration at 25 °C. For cyclic voltammetry (CV) and square wave voltammetry (SWV), the working electrode was a platinum (Pt) disk with a surface area of 0.071 cm^2. The surface of the working electrode was polished with a diamond suspension before each run. A Pt wire served as the counter electrode. Saturated calomel electrode (SCE) was employed as the reference electrode and separated from the bulk of the solution by a double bridge. Ferrocene was used as an internal reference. Tetrabutylammonium perchlorate (TBAP) in DCM and DMSO was employed as the supporting electrolyte at 0.10 mol dm^{-3}. High purity N_2 was used to remove dissolved O_2 at least 15 min prior to each run and to maintain a nitrogen blanket during the measurements. IR compensation was applied to the CV and SWV scans to minimize the potential control error.

UV/Vis absorption spectra were measured by an OceanOptics QE65000 diode array spectrophotometer. *In situ* spectroelectrochemical measurements were carried out by utilizing a three-electrode configuration of thin-layer quartz spectroelectrochemical cell at 25 °C. The working electrode was a semi-transparent Pt tulle. A Pt wire counter electrode and a SCE reference electrode separated from the bulk of the solution by a double bridge were used.

The EPR spectra were recorded with a Varian E-109C X-band spectrometer. The magnetic field modulation frequency was 100 kHz, and the microwave power was 10 mW. Samples were inserted in quartz tubes (3–4 mm). The g-values were obtained by comparison with a diphenylpicrylhydrazyl (DPPH) sample of $g = 2.0036$. The X-band EPR powder spectra of all complexes were recorded at 298 K and in frozen DMF (113 K).

2.3. *Synthesis of the half unit, 2-hydroxy naphtylidene-3,4-diaminobenzophenone (NADAB)*

A solution of 0.01 mol of DAB dissolved in 10 mL of methanol was added to a stirred solution of 2-hydroxy-1-naphthaldehyde (0.01 or 0.02 mol in 10 mL of methanol). The

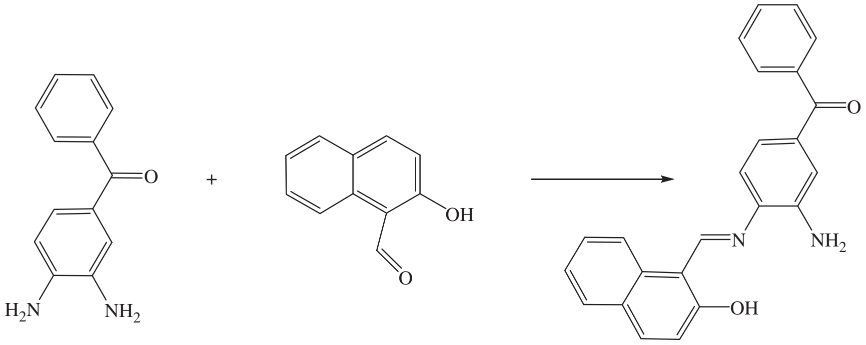

Figure 1. Synthesis of the half unit (NADAB).

reaction mixture was refluxed with stirring for 3 h. The resulting precipitate was filtered off and washed with cold methanol. The product was finally recrystallized from methanol to get an orange solid with a yield of 85% (figure 1).

2.4. *Synthesis of the metal complexes*

2.4.1. Template synthesis of the unsymmetrical diimino VO(IV) and Cu(II) complexes. *Synthesis of 3-naphthylidene-4-salicylidene-diaminobenzophenone oxovanadium(IV)* ***(1)***. A total of 0.06 g of NADAB was dissolved in DCM. To this solution, 0.008 mL salicylaldehyde was added and heated. Then, 0.03 g of $VOSO_4{\cdot}H_2O$ solution in 10 mL of ethanol was added to the ligand solution and the mixture was allowed to stir at 60–70 °C for 2 h. Green precipitates were obtained and dried with P_2O_5 for 12 h at vacuum. The purity was controlled by thin layer chromatography (TLC). Complexes **2** and **3** were synthesized in a similar manner (figure 2).

Synthesis of 3-naphthylidene-4-salicylidene-diaminobenzophenone copper(II) ***(4)***. A total of 0.07 g of NADAB was dissolved in DCM, and 0.02 mL of salicylaldehyde was added. After 0.04 g of $Cu(CH_3COO)_2$ solution in 10 mL of ethanol was added to ligand solution, the mixture was allowed to stir at 60 °C for 2 h. Brown precipitates were obtained and dried

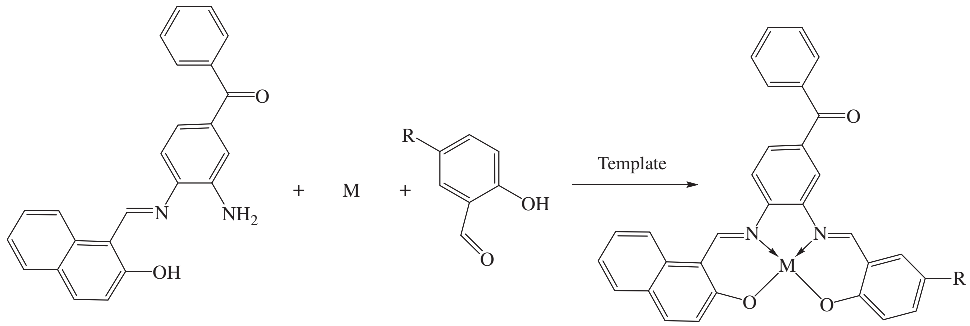

M/R: VO(IV)/H (**1**), VO(IV)/Cl (**2**), VO(IV)/Br (**3**), Cu(II)/H (**4**), Cu(II)/Cl (**5**), Cu(II)/Br (**6**)

Figure 2. Synthesis of metal complexes by template effect of metal ions.

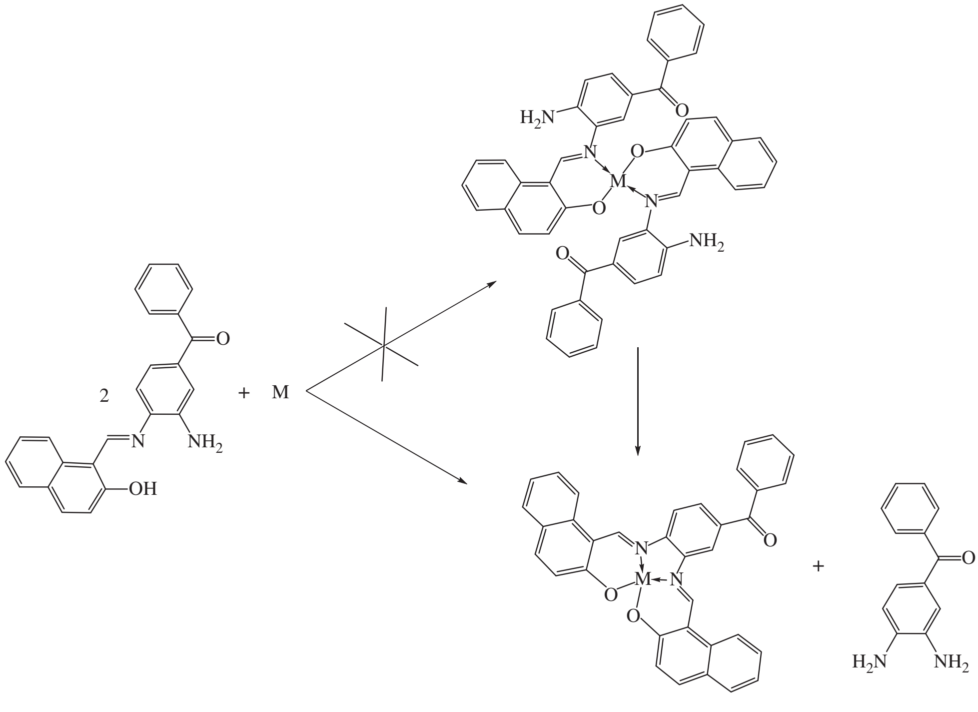

M: VO(IV) (**7**), Cu(II) (**8**)

Figure 3. Synthesis of symmetrical metal complexes by rearrangement of (NADAB).

with P_2O_5 for 12 h at vacuum. The purity was controlled by TLC. Complexes **5** and **6** were synthesized in a similar manner. The template synthesis of complexes is shown in figure 2.

2.4.4. Synthesis of the symmetrical diimino VO(IV) and Cu(II) complexes derived from NADAB. *Synthesis of 3,4-bis(naphthylidene)-diaminobenzophenone oxovanadium (IV) (7) and Cu(II)* ***(8)***. A total of 0.10 g of NADAB was dissolved in 15 mL of DCM. The second aldehyde was added to this solution. After the mixture was allowed to stir at 60 °C for 2 h, 0.04 g of $VOSO_4{\cdot}H_2O$ solution in 10 mL of ethanol was added. Green precipitates were obtained and dried with P_2O_5 for 12 h at vacuum. The purity was controlled by TLC. The same preparation scheme was repeated with Cu(II) complex (**8**) (figure 3).

2.4.6. *In situ* synthesis of the symmetrical diimino VO(IV) and Cu(II) complexes. *Synthesis of 3,4-bis(5-chlorosalicylidene)-diaminobenzophenone oxovanadium(IV)* ***(9)***. A total of 0.17 g of DAB was dissolved in 15 mL of DCM. To this solution, 0.26 g of 5-chlorosalicylaldehyde was added. After the mixture was allowed to stir at 60 °C for 2 h, 0.13 g of $VOSO_4{\cdot}H_2O$ solution in 10 mL of ethanol was added. Green precipitates were obtained and dried with P_2O_5 for 12 h at vacuum. The purity was controlled by TLC. Complex **10** was synthesized in a similar manner (figure 4).

Synthesis of 3,4-bis(5-chlorosalicylidene)-diaminobenzophenone copper(II) ***(11)***. A total of 0.17 g of DAB was dissolved in 20 mL of DCM. To this solution, anhydrous Na_2SO_4

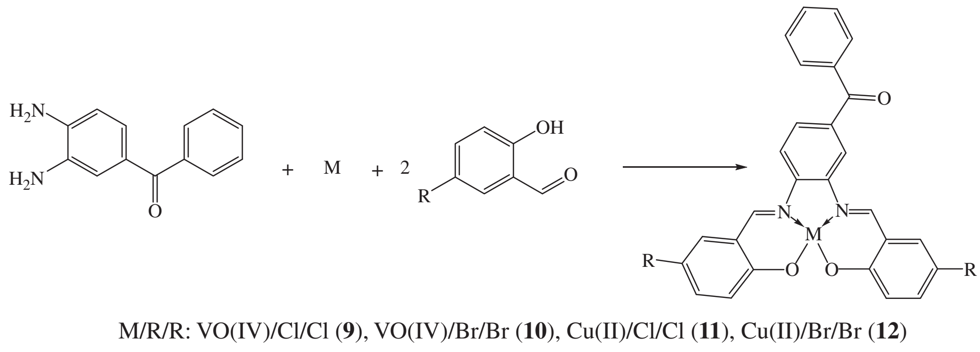

Figure 4. *In-situ* synthesis of symmetrical metal complexes.

was added. After the mixture was allowed to stir at room temperature for 4–5 h, it was filtered; 0.26 g of 5-chlorosalicylaldehyde was added to this solution and stirred for one hour. A total of 0.16 g of $Cu(CH_3COO)_2$ solution in 10 mL of ethanol was added, and the reaction mixture was allowed to precipitate by stirring at room temperature. Brown precipitates were obtained and dried with P_2O_5 for 12 h at vacuum. The purity was controlled by TLC. Complex **12** was synthesized in a similar manner (figure 4).

The results of analytical and spectroscopical characterization of the half unit and all complexes are as follows.

Compound: color, m.p. (°C), yields (%), formula (molecular weight) elemental analysis in C, H, N% given as found (calculated); infrared bands (KBr disk, cm^{-1}), and ^{1}H-NMR chemical shifts (in $CDCl_3$, ppm).

NADAB: orange, 123–124 °C, 85%, Found (Calcd) for $C_{24}H_{20}N_2O_2$ (368.43 g/mol): C, 78.11 (78.24); H, 6.62 (6.47); N, 7.21 (7.60)%. IR: υ(OH) 3492, $\upsilon_s(NH_2)$ 3346, $\upsilon_{as}(NH_2)$ (s) 3106, δ(N–H) 1646, υ(C=N) 1607, υ(C–O) 1176. ^{1}H-NMR: 14.65 (s, 1H, OH), 9.45 (s, 1H, CH), 4.5 (s, 2H, NH_2), 6.72–8.14 (aromatic protons, 13 H).

Complexes:

1: light green, >300 decomp., 65. Found (Calcd) for $C_{31}H_{20}N_2O_4V$ (535.44 g/mol): C, 58.56 (58.51); H, 6.62 (6.91); N, 17.21 (17.15)%. IR: υ υ(C=O) 1659 s, υ(C=N) 1601 s, 1578 s, υ(C=C) 1531 s, phenolic υ(C–O) 1197 s, υ(C–H) 3056 w, 3041 w, υ(V=O) 977 s.

2: light green, >300 decomp., 60. Found (Calcd) for $C_{31}H_{19}N_2ClO_4V$ (569.88 g/mol): C, 65.77 (65.33); H, 3.52 (3.36); N, 4.21 (4.92)%. IR: υ(C=O) 1661 s, υ(C=N) 1607 s, 1576 s, υ(C=C) 1538 s, phenolic υ(C–O) 1200 s, υ(C–H) 3061 w, υ(V=O) 984 s.

3: light green, >300 decomp., 58. Found (Calcd) for $C_{31}H_{19}N_2BrO_4V$ (614.34 g/mol): C, 60.56 (60.61); H, 6.52 (6.91); N, 4.16 (4.56)%. IR: υ(C=O) 1661 s, υ(C=N) 1607 s, 1576 s, υ(C=C) 1538 s, phenolic υ(C–O) 1200 s, υ(C–H) 3053 w, υ(V=O) 984 s.

4: brown, >300 decomp., 54. Found (Calcd) for $C_{31}H_{20}N_2O_3Cu$ (532.04 g/mol): C, 69.56 (69.98); H, 3.62 (3.79); N, 5.21 (5.27)%. IR: υ(C=O) 1653 s, υ(C=N) 1607 s, 1584 s, υ(C=C) 1538 s, phenolic υ(C–O) 1192 s, υ(C–H) 3061.

5: brown, >300 decomp., 58. Found (Calcd) for $C_{31}H_{19}N_2ClO_3Cu$ (566.49 g/mol): C, 65.56 (65.73); H, 3.62 (3.38); N, 4.21 (4.95)%. IR: υ(C=O) 1661 s, υ(C=N) 1615 s, 1584 s, υ(C=C) 1538 s, phenolic υ(C–O) 1192 s, υ(C–H) 3053.

6: brown, >300 decomp., 60. Found (Calcd) for $C_{31}H_{19}N_2BrO_3Cu$ (610.94 g/mol): C, 60.56 (60.94); H, 3.52 (3.13); N, 4.65 (4.59)%. IR: υ(C=O) 1661 s, υ(C=N) 1607 s, 1584 s, υ(C=C) 1538 s, phenolic υ(C–O) 1192 s, υ(C–H) 3053.

7: light green, >300 decomp., 65. Found (Calcd) for $C_{35}H_{24}N_2O_4V$ (587.52 g/mol): C, 71.66 (71.55); H, 4.62 (4.12); N, 4.71 (4.77)%. IR: υ(C=O) 1659 s, υ(C=N) 1616 s, 1601 s, υ(C=C) 1574 s, phenolic υ(C–O) 1200 s, υ(C–H) 3056 w, υ(V=O) 977 s.

8: brown, >300 decomp., 65. Found (Calcd) for $C_{35}H_{26}N_2O_3Cu$ (582.10 g/mol): C, 71.56 (71.72); H, 4.62 (4.47); N, 4.89 (4.78)%. IR: υ(C=O) 1661 s, υ(C=N) 1615 s, 1584 s, υ(C=C) 1538 s, phenolic υ(C–O) 1192 s, υ(C–H) 3056.

9: light green, >300 decomp., 60. Found (Calcd) for $C_{27}H_{16}N_2Cl_2O_4V$ (554.27 g/mol): C, 58.56 (58.51); H, 6.62 (6.91); N, 17.21 (17.15)%. IR: υ(C=O) 1659 s, υ(C=N) 1612 s, 1585 s, υ(C=C) 1524 s, phenolic υ(C–O) 1185 s, υ(C–H) 3083 w, 3052 w, υ(V=O) 981 s.

10: light green, >300 decomp., 55. Found (Calcd) for $C_{27}H_{16}N_2Br_2O_4V$ (643.17 g/mol): C, 58.56 (58.42); H, 2.62 (2.51); N, 4.21 (4.36)%. IR: υ(C=O) 1655 s, υ(C=N) 1605 s, 1582 s, υ(C=C) 1516 s, phenolic υ(C–O) 1181 s, υ(C–H) 3079 w, 3048 w, υ(V=O) 981 s.

11: dark brown, 360–361, 55. Found (Calcd) for $C_{27}H_{16}N_2Cl_2O_3Cu$ (550.88 g/mol): C, 58.43 (58.87); H, 2.62 (2.91); N, 5.21 (5.09)%. IR: υ(C=O) 1651 s, υ(C=N) 1608 s, 1574 s, υ(C=C) 1512 s, phenolic υ(C–O) 1173 s, υ(C–H) 3056.

12: dark brown, 347–348, 60. Found (Calcd) for $C_{27}H_{16}N_2Br_2O_3Cu$ (639.78 g/mol): C, 50.56 (50.69); H, 2.62 (2.52); N, 4.21 (4.38)%. IR: υ(C=O) 1651 s, υ(C=N) 1608 s, 1578 s, υ(C=C) 1508 s, phenolic υ(C–O) 1177 s, υ(C–H) 3056.

3. Results and discussion

The half unit, NADAB (HL), was synthesized from 2-hydroxy-1-naphthaldehyde and DAB, in both 1 : 1 and 2 : 1 M ratios in methanolic solution (figure 1). The reaction of this half unit with appropriate aldehydes did not give the asymmetrical Schiff bases in methanolic solution. The VO(IV) and Cu(II) complexes (**1–6**) of asymmetrical Schiff bases were prepared according to a template method by condensation of the half unit (HL) with other aldehydes in the presence of VO(IV) and Cu(II), in 1 : 1 : 1 mole ratio (figure 2).

2-Hydroxy naphthylidene diimine complexes were obtained from complexation of NADAB with metal ions while monoimine complexes were expected (figure 3). Reactions of metal ions with NADAB in methanolic solution led to formation of the symmetrical diimino complexes via elimination of a diamine molecule.

VO(IV) and Cu(II) complexes of symmetrical Schiff base derived from 5-chlorosalicylaldehyde or 5-bromosalicylaldehyde were prepared according to a direct method by condensation of the aldehydes with diamine and then with addition of Cu(II) or VO(IV) in 2 : 1 : 1 mole ratio without isolation of the symmetrical Schiff bases (figure 4).

The structures of the complexes were confirmed by elemental analysis, FTIR and ESI-Mass spectroscopy. Elemental analyses, NMR and IR spectroscopy, UV–Vis spectrophotometry, and conductivity measurements were used to confirm the syntheses of the half unit and complexes. All VO(IV) and Cu(II) complexes are colored, stable in air and non-hygroscopic solids. These complexes are soluble in DMF and DMSO. Elemental analysis shows that all the complexes have 1 : 1 stoichiometry, ML. The molar conductance values are too low (6–14 $\Omega^{-1}\,\mathrm{cm}^2\,\mathrm{mol}^{-1}$) to account for dissociation of the complexes in DMF or DMSO. Hence, these complexes can be regarded as non-electrolytes [38]. The results of elemental analyses and physical properties of the half unit and complexes are listed in the Experimental section.

3.1. *IR spectra*

Important infrared absorptions of the half unit ligand and the complexes and their assignments are given in the Experimental section. The IR spectra of the half unit exhibit two sharp and strong bands at 3397 and 3381 cm^{-1}, assignable to the primary amine stretches. These two bands are not observed in spectra of the complexes.

The half unit ligand shows a strong band corresponding to υ(C=N) at 1610–1630 cm^{-1} with a remarkable shift to lower wavenumbers upon complexation, which indicates participation of N in coordination, arising from shift of electron density from nitrogen to metal, lowering the stretching frequency of the corresponding vibration.

The band of (O–H) is also absent in the complexes, showing loss of hydrogen upon complexation. Coordination of the ligand is further supported by bands around 1250 cm^{-1} which shift to higher wavenumbers of υ(C–O) in the complexes, probably due to formation of C–O–M.

All the oxovanadium(IV) complexes exhibit a strong band at 959–988 cm^{-1}, assigned to v(V=O) with a monomeric square pyramidal coordination geometry [39, 40].

The crystal structures of some of the VO(II) and Cu(II) salen complexes have been reported [41, 42]. In this study, we could not manage to obtain suitable crystals for X-ray diffraction analyses.

3.2. *UV–Visible spectra*

The electronic spectrum of the half unit shows two bands at 343 and 425 nm assigned to $\pi\to\pi^*$ and $n\to\pi^*$ transitions involving the C=N chromophore. In the visible spectra of the metal complexes, these bands shift to higher wavelengths. The oxovanadium complexes (**7**, **9,** and **10**) have two bands at 348–352 nm and 432 nm which can be attributed to $\pi\to\pi^*$

Table 1. The electronic spectral data of the Schiff base (L) and metal complexes (nm) in DMSO.

Compound	$\pi\to\pi^*$	$n\to\pi^*$	MLCT
NADAB	343	425	
1	314	426	
2	314	426	
3	327	425	469sh
4	315, 350sh	442	
5	315, 349sh	442	
6	329, 349sh	435	485sh
7	348	432	476sh
8	327, 348sh	435	485sh
9	351	432	476sh
10	352	432	478sh
11	327, 349sh	435	485sh
12	327, 348sh	436	491sh

and $n \rightarrow \pi^*$ transitions. Some oxovanadium complexes have a shoulder at 469–478 nm which can be assigned to metal to ligand charge transfer (MLCT). When compared with free L, visible spectra of the copper complexes (**4**, **5**, **6**, **8**, **11** and **12**) have higher wavelengths at 315–327 nm (including a shoulder at 348–350 nm), 435–442 nm, and 485–491 nm as a shoulder assigned to $\pi \rightarrow \pi^*$, $n \rightarrow \pi^*$, and MLCT transitions, respectively. The d–d bands were not observed for oxovanadium or copper complexes (table 1).

3.3. *Mass spectra*

Mass spectra were obtained for **7** and **9**. The ES-Mass spectrum of VO(IV) complex (**9**) shows the $(M-1)^+$ peak corresponding to molecular ion with 100% relative abundance. In addition, the spectrum of **9** has $(M+1)^+$: 555.47. In a similar manner, **7** has a peak corresponding to molecular ion (587.52 g/mol) with 16% relative abundance as well as $(M-1)^+$: 586.70 (52.04%); $(M-2)^+$: 585.70 (100.00%) peaks (Supplementary material).

Table 2. Voltammetric data of the investigated compounds in DCM/TBAP electrolyte on Pt working electrode versus SCE reference electrode.

Complex		$V^{IV}O/V^{V}O$	Ligand red.
9	${}^{a}E_{1/2}$ *vs.* SCE	0.70	−0.99
	${}^{b}\Delta E_p$ (mV)	60	98
	${}^{c}I_{pa}/I_{pc}$	0.98	0.45
10	${}^{a}E_{1/2}$ (V)	0.71	−0.98
	${}^{b}\Delta E_p$ (mV)	62	82
	${}^{c}I_{pa}/I_{pc}$	0.96	0.42
7	${}^{a}E_{1/2}$	0.73	−0.95
	${}^{b}\Delta E_p$ (mV)	81	70
	${}^{c}I_{pa}/I_{pc}$	0.90	0.40
1	${}^{a}E_{1/2}$ *vs.* SCE	0.72	−0.97
	${}^{b}\Delta E_p$ (mV)	75	71
	${}^{c}I_{pa}/I_{pc}$	0.92	0.46
2	${}^{a}E_{1/2}$ (V)	0.75	−0.96
	${}^{b}\Delta E_p$ (mV)	80	80
	${}^{c}I_{pa}/I_{pc}$	0.95	0.44
11	${}^{a}E_{1/2}$	–	−1.05
	${}^{b}\Delta E_p$ (mV)	–	70
	${}^{c}I_{pa}/I_{pc}$	–	0.46
12	${}^{a}E_{1/2}$	–	−0.95
	${}^{b}\Delta E_p$ (mV)	–	62
	${}^{c}I_{pa}/I_{pc}$	–	0.42
6	${}^{a}E_{1/2}$	–	−0.88
	${}^{b}\Delta E_p$ (mV)	–	65
	${}^{c}I_{pa}/I_{pc}$	–	0.56
4	${}^{a}E_{1/2}$	–	−0.96
	${}^{b}\Delta E_p$ (mV)	–	66
	${}^{c}I_{pa}/I_{pc}$	–	0.67

[a] $E_{1/2} = (E_{pa} + E_{pc})/2$ at 0.100 Vs^{-1}.

[b] $\Delta E_p = E_{pa} + E_{pc}$ at 0.100 Vs^{-1}.

[c] I_{pa}/I_{pc} for reduction, I_{pc}/I_{pa} for oxidation processes at 0.100 Vs^{-1} scan rate.

3.4. *Electrochemical studies*

To investigate the effects of substitutions on the redox properties of VO(IV) and Cu(II) complexes, voltammetric experiments were carried out in DCM/TBAP and DMSO/TBAP electrolyte systems at room temperature. table 2 lists the assignments of the redox couples and the electrochemical parameters of the complexes, which included the half-wave peak potentials ($E_{1/2}$), anodic to cathodic peak potential separation (ΔE_p), and ratio of the anodic to cathodic peak currents (I_{pa}/I_{pc}). $E_{1/2}$ values are in agreement with reported data for redox processes in similar O–N–S complexes in the literature [43–47]. Different metallo–salen complexes have been reported [46–48]. These complexes generally give only metal-based electron transfer processes. For instance, Tsuchida and coworkers reported that [VOL] gave an oxidation couple at 0.44 V assigned to the $V^{IV}OL/V^{V}OL$ process [46]. Similarly, Maeda and coworkers reported different [VOL] complexes, which gave $V^{IV}OL/V^{V}OL$ between 0.70 and 1.10 V depending on the substituents of the ligands [47]. Kraemer and his coworkers reported the redox properties of VO and Cu-salen complexes with $E_{1/2}$ between +0.52 and +0.48 V for V^{V}/V^{IV} of VO salen complexes and between −0.80 and −1.08 V for Cu^{II}/Cu^{I} half reactions of copper salen complexes [48]. In our study, while Cu(II) complexes give only a ligand-based reduction, VO(IV) complexes give a metal-based oxidation process in addition to the ligand-based reduction. Changing the salen ligand with naphthalene shifts the redox processes, however, Cl, Br, and OH groups on the ligands do not affect the redox behavior.

Electrochemical analysis of Cu(II) complexes was performed in DCM/TBAP and DMSO/TBAP electrolyte systems and redox responses of these complexes were compared with the similar complexes [48]. All Cu(II) complexes give a reduction process at −1.0 V. As shown in table 2, the only difference between the Cu(II) complexes is shift of the reduction slightly and changing the reversibility of the process from different electron-donating ability of the substituents. Cu(II) complexes bearing two salen units generally give an irreversible reduction. A typical CV and SWV of **11** are depicted in Supplementary Material as a representative example. Complex **11** gives a reduction couple (**R_1**) at −1.05 V. Even though ΔE_p values of (65 mV at 100 mVs^{-1} scan rate) **11** were in reversible range especially at very slow scan rates, small I_{pa}/I_{pc} values (0.45 at 100 mVs^{-1} scan rate) and deviation of I_p *versus* $v^{1/2}$ from linearity indicate irreversible redox to the chemical reactions succeeding the electron transfer processes. Due to the chemical reactions succeeding the reduction redox process, CVs of **11** give an oxidation wave (**CP_1**) at −0.25 V assigned to chemical reaction products during the reverse potential scans. Changing the vertex potential clearly indicates the presence of the chemical reaction succeeding the **R_1** process. While there is no wave at −0.25 V, when the potential is switched before the **R_1** process, **CP_1** wave is recorded when the switching potential passed the **R_1** process. During continuous scans, while the peak current of the **R_1** decreases, the peak current of **CP_1** increases, which support this chemical reaction. To investigate the effect of solvent, CV and SWV of the complexes were also recorded in DMSO. CV and SWV of **11** in DMSO (Supplementary material) are recorded at different scan rates. The complex gives very similar redox responses in both DCM and DMSO. The only difference is the shifting of the reduction to negative due to electron-donating ability of DMSO. **11** gives a chemically irreversible reduction couple, **R_1**, at −1.14 V and a **CP_1** process at −0.34 V.

Swapping the salen unit with naphthalene increases the reversibility of the reduction process of the Cu(II) complexes. CV and SWV responses of **4** in DCM/TBAP electrolyte system are provided in Supplementary material. **4** gives a reduction couple (**R_1**) at −0.96 V.

ΔE_p values of (80 mV at 100 mVs^{-1} scan rate) **4** indicate the electrochemical reversibility of the process especially at very slow scan rates. I_{pa}/I_{pc} values are very small at slow scan rates (0.45 at 100 mVs^{-1} scan rate), however, I_{pa}/I_{pc} values increase with the scan rates (0.75 at 1000 mVs^{-1} scan rate). When compared with **11**, the presence of naphthalene increases the chemical reversibility and stability of the complex with respect to I_{pa}/I_{pc} and I_p *versus* $v^{1/2}$ changes. Complex **4** also gives a **CP$_1$** process at −0.13 V, but the peak current of this process is much smaller than that of **11**, which also supports the stability of **4**.

In situ spectroelectrochemical studies were employed to determine spectra of electrogenerated Cu(II) complexes. There are no studies on spectroelectrochemical characterization of salen complexes. Thus, spectra of electrogenerated species of the salen complexes are reported for the first time in this study. We assigned redox processes by comparing spectral changes of salen-type complexes with similar N_2O_2-Schiff bases in the literature [49–51]. The initial spectrum under open circuit potential is dominated by metal-to-ligand charge transfer (MLCT at 470 nm with a shoulder at 497 nm) and intraligand transitions ($\pi \rightarrow \pi^*$ transition at 298 nm; $n \rightarrow \pi^*$ transition at 394 nm). All Cu(II) complexes exhibited similar spectral changes under the applied potential during the spectroelectrochemical measurements. Thus, *in situ* UV–Vis spectral changes of **11** as a representative of the Cu(II) complexes (Supplementary material) with applied potential at −1.20 V, the ligand to metal charge transfer (LMCT) band at 497 nm decreases in intensity without shift, while the intraligand transitions at 397 and at 470 nm remain unchanged. A broad new band is observed at 545 nm. Unchanged intraligand transitions and observation of a new LMCT band at 545 nm indicate a ligand-based redox process assigned to $[Cu^{II}L]/[Cu^{II}L^{-1}]^{-1}$. Oscillation in isosbestic points at 500 nm demonstrates that the reduction proceeds to give more than a single, reduced species. This behavior supports the presence of chemical reaction after reduction for Cu(II)L complexes.

Electrochemical analyses of VO(IV) complexes were also performed in DCM/TBAP and DMSO/TBAP electrolyte systems and redox responses compared with those of similar complexes. All VO(IV) complexes give a reduction process at −1.0 V and a reversible oxidation couple at 0.70 V. Changing the salen unit with naphthalene shifts the redox potentials to the positive. Changing the substituents on the salen units did not appreciably affect the redox behavior of the complexes. DMSO instead of DCM as the solvent just shifts the redox processes to the negative and did not affect the redox behavior. CV and SWV responses of **9** are provided in Supplementary material. On cathodic potentials, the complex gives a chemically irreversible reduction (**R$_1$**) at −0.99 V ($\Delta E_p = 70$ mV and $I_{pa}/I_{pc} = 0.35$ at 100 mVs^{-1} scan rate). Due to the chemical reactions succeeding the reduction, CVs of **9** give an oxidation wave (**CP$_1$**) at −0.10 V assigned to the chemical reaction products during the reverse scans. In addition to the reduction, **9** gives a reversible oxidation couple at 0.70 V, assigned to $V^{IV}O/V^{V}O$, when compared with redox responses of Cu(II) complexes and VO(IV) complexes in the literature. *In situ* spectroelectrochemical measurements (discussed below) were also used to confirm this assignment. To illustrate the effect of naphthalene, CV and SWV responses of **2** (Supplementary material) show changing the 5-chloro salicylidene unit with 2-OH-naphthylidene shifts the redox processes positive about 0.40 V. Complex **9** gives an irreversible reduction at −0.95 V and an oxidation couple at 0.74 V.

When reduction responses of **9** are compared with **11**, both complexes give very similar reduction at the same potential, indicating that this process is due to the ligands, not to the metal center. It is reported that Cu–salen complexes gave similar reduction processes, assigned to reduction of Cu^{II} to Cu^{I} [49–51]. Comparison of VO(IV) and Cu(II) in this study, however, indicates that all complexes give a reduction at similar potentials with similar properties without regarding to the metal. Thus, the reduction of Cu(II) is proposed as a ligand-based process. This assignment was confirmed with the *in situ* spectroelectrochemical measurements discussed above.

In situ spectroelectrochemical studies were employed to determine the spectra of electrogenerated species of the VO(IV) complexes and to assign the redox processes in the CVs of the complexes. Supplementary material provides *in situ* UV–Vis spectral changes of **9** as a representative of VO(IV) complexes during controlled potential reductions and oxidation. Under applied potential at −1.20 V, the broad MLCT band at 465 nm decreases in intensity without shift and a new band is recorded at 575 nm, while the $\pi \rightarrow \pi^*$ transition band at 304 nm decreases slightly. At the same time, the $n \rightarrow \pi^*$ transition bands at 410 nm increase in intensity with blue shift. Well-defined isosbestic points at 350 and 413 nm demonstrate that the reduction proceeds to give a single, reduced species. Decreasing the $\pi \rightarrow \pi^*$ transition without a shift and observation of a new MLCT band characterize a ligand-based electron transfer reaction for metal complexes. Spectroscopic changes illustrate the spectral changes during oxidation. While the bands at 430 and 360 nm decrease in intensity shifting to blue, two new bands are recorded at 360 and 650 nm. These spectral changes indicate a metal-based oxidation, assigned to the $V^{IV}O/V^{V}O$ process.

3.5. *EPR investigation of complexes*

X-band EPR powder spectra of the salen-type oxovanadium(IV) complexes were recorded at room temperature. A broad band for **7** (Supplementary material) is observed for which $g_{iso} = 1.986 \pm 0.0005$. The EPR spectra of oxovanadium(IV) complexes derived from DAB in the polycrystalline state at 298 K show only one broad signal at $g_{iso} = 1.9845$ for **10**, 1.986 for **7**, 1.9831 for **1**, 1.9933 for **2,** and 1.980 for **3**, respectively.

EPR spectra provide information about the coordination environment around copper(II) [52]. The EPR spectra of **6** and **5** in the polycrystalline state at 298 K show only one broad signal at $g_{iso} = 2.077$ and 2.0996, respectively. Such isotropic spectra, consisting of only one broad signal and hence only one g value (g_{iso}), arise from extensive exchange coupling through misalignment of the local molecular axes between different molecules in the unit cell (dipolar broadening) and enhanced spin lattice relaxation. This type of spectrum gives no information on the electronic ground state of the copper(II) in the complexes [52].

The powder EPR spectrum of **8** was recorded at 298 K (Supplementary material). Only one $g_{||}$ and $g_{\perp}$ components were obtained, due to the influence of exchange interactions which makes the hyperfines smaller. The powder EPR spectra of **11**, **12,** and **4** were also recorded at 298 K. The powder EPR spectra of **11**, **12**, **4,** and **8** show axial spectra with well-defined $g_{||}$ and $g_{\perp}$ features. The obtained values are $g_{||} = 2.184$, $g_{\perp} = 2.058$ for **11**; 2.195 and 2.058 for **12**; 2.139 and 2.049 for **4**; 2.177 and 2.043 for **8**, respectively. The variation in $g_{||}$ and $g_{\perp}$ values indicates that the geometry of the compounds in the solid state is affected by coordinating anions [52].

The geometric parameter G, which is a measure of the exchange interaction between copper centers, is calculated for **11**, **12**, **4,** and **8** using the equation: $G = (g_{||} - 2.0023)/(g_{\perp} - 2.0023)$ [53–56]. For $3.0 < G < 5.0$, the exchange interaction (coupling) is considered to be weak and in such cases the g-values reflect the local Cu(II) environment. On the other hand, $G < 3.0$ indicates strong exchange coupling and the observed g-values do not reflect the individual Cu(II) molecular geometry [36]. G-values < 4.4 are consistent with a d_{x2-y2} ground state having a small exchange coupling [52, 57]. If $G > 4$, the exchange

Table 3. Anisotropic EPR spectral data for some Cu(II) complexes.

Compound	T (K)	$g_{\|}$	$g_{\perp}$	$A_{\|}$ (cm^{-1})	$g_{\|}/A_{\|}$ (cm^{-1})	G	α^2	References
11	113	2.184	2.0448	188G	116	4.275	0.7614	This work
12	113	2.1925	2.0446	192G	114	4.496	0.78099	This work
6	113	2.1897	2.045	191G	114	4.430	0.7751	This work
5	113	2.178	2.047	185G	118	3.930	0.7480	This work
4	113	2.1925	2.0495	193G	114	4.029	0.7858	This work
8	113	2.189	2.047	193G	113	4.177	0.7813	This work
$Cu(L^2)_2$		2.229	2.057	174	137	4.02	0.50	[52]
$Cu(L^8)_2$		2.211	2.046	184	127	4.58	0.50	[52]
$Cu(L^9)_2$		2.231	2.048	166	144	4.37	0.52	[52]
$Cu(L^{12})_2$		2.226	2.042	166	143	5.38	0.52	[52]
$[Cu(enc)_2(sac)_2(H_2O)]\cdot 1.44H_2O$	77	2.296	2.060	150	–	–	0.7716	[34]

A values in $10^{-4}\,cm^{-1}$.

interaction is negligible [58]. $g_{\|} > g_{\perp}$ and a G of 2.1–3.8 are consistent with a d_{x2-y2} ground state for **11**, **12**, **4,** and **8** (table 3).

The EPR spectrum of **8** in frozen DMF solution at 113 K has four line hyperfine patterns arising from the $g_{\|}$ region of copper(II). The symmetry of paramagnetic center is axial: $g_{\|} = 2.193$, $g_{\perp} = 2.049$, $A_{\|} = 193 \times 10^{-4}\,cm^{-1}$. The ratio $g_{\|}/A_{\|}$ can be used to predict the geometry adopted by copper complexes; these values of 113–116 indicate a distorted square-planar geometry around copper. In square-planar complexes, this parameter is from 105 to 135 cm, whereas the value falls to 135–258 cm for distorted tetrahedral complexes [37, 59]. The EPR parameters $g_{\|}$, $g_{\perp}$, $A_{\|}$ of **11**, **12**, **4,** and **8** were used to evaluate the bonding parameters α^2, which may be regarded as measures of the covalency in the in-plane σ-bonds. The value of in-plane σ-bonding parameter α^2 is estimated from the expression [36]:

$$\alpha^2 = A_{\|}/0.036 + (g_{\|} - 2.0023) + 3/7(g_{\perp} - 2.0023) + 0.04 \qquad (1)$$

The parameter was 0.748–0.785 (table 3) and indicates the presence of significant in-plane σ-bonding in **11**, **12**, **4,** and **8** [36, 56]. Because the values of α^2 are less than 1.0 expected for 100% ionic character of bonding, the in-plane σ-bond has ionic character for **11**, **12**, **4,** and **8** [60]. The EPR spectra for **11**, **12**, **4,** and **8** in DMF solution at 113 K are characterized by axially symmetric ***g*** and ***A*** tensors with $g_{\|} > g_{\perp}$ and $A_{\|} > A_{\perp}$ (table 3) in solution, suggesting that the unpaired electron occupies d_{x2-y2} orbital. This result is in agreement with crystal structures [61, 62].

4. Conclusion

The half unit, NADAB, VO(IV) and Cu(II) complexes (**1–12**) were synthesized and characterized. The metal is coordinated through the azomethine nitrogens and phenolic oxygens via deprotonation. The bonding to metal is confirmed by analytical and spectral studies. Voltammetric and spectroelectrochemical studies show that while Cu(II) complexes give one-electron reduction processes, VO(IV) complexes give irreversible ligand-based reduction and a reversible metal-based oxidation. Redox potentials of the complexes shift to positive potentials when salicylidene is changed with naphthylidene. Reversible oxidation properties of VO(IV) complexes at less positive values indicate their possible electrocatalytic and electrochemical sensor applications. Determination of the spectra of the electrogenerated anionic and cationic form of the complexes is important to decide their possible spectroscopic applications.

EPR spectra of the Cu(II) complexes in frozen DMF at 113 K indicated distorted square-planar geometry. The EPR spectra of Cu(II) complexes at 113 K are characterized by axially symmetric **g** and **A** tensors with $g_{\|} > g_{\perp}$ and $A_{\|} > A_{\perp}$ in solution, suggesting that the unpaired electron occupies a formal d_{x2-y2} orbital.

References

[1] S. Mohebbi, D.M. Boghaei, A.H. Sarvestani, A. Salimi. *Appl. Catal. A: Gen.*, **278**, 263 (2005).
[2] D.M. Boghaei, S. Mohebbi. *Tetrahedron*, **58**, 5357 (2002).
[3] M. Asadi, S.B. Sadi, Z. Asadi, R. Yousefi, A.R.B. Sadi, H. Khalili-Hezarjaribi. *J. Coord. Chem.*, **65**, 722 (2012).
[4] N. Daneshvar, A.A. Entezami, A.A. Khandar, L.A. Saghatforoush. *Polyhedron*, **22**, 1437 (2003).
[5] N. Durai, G.J. Saminathan. *Clin. Biochem. Nutr.*, **22**, 31 (1997).
[6] I. Correia, J. Costa Pessoa, M.T. Duarte, R.T. Henriques, M.F.M. Piedade, L.F. Veiros, T. Jakusch, A. Dörnyei, T. Kiss, M.M.C.A. Castro, C.F.G.C. Geraldes, F. Avecilla. *Chem. Eur. J.*, **10**, 2301 (2004).
[7] H. Sigel, A. Sigel. *Vanadium and Its Role in Life. In Metal Ions in Biological Systems*, Marcel Dekker, New York, NY (1995).
[8] A.S. Tracey, D.C. Crans. *Vanadium Compounds. In Chemistry, Biochemistry and Therapeutic Applications*, American Chemical Society, Washington, DC (1998).
[9] S. Liang, D.V. Derveer, S.Y. Qianc, B. Sturgeon, X.R. Bu. *Polyhedron*, **21**, 2021 (2002).
[10] D. Rehder. *Angew. Chem. Int. Ed. Engl.*, **30**, 148 (1991).
[11] A. Butler, C.J. Carrano. *Coord. Chem. Rev.*, **109**, 152 (1991).
[12] C.J. Chang, J.A. Labinger, H.R. Gray. *Inorg. Chem.*, **36**, 5927 (1997).
[13] B.J. Hamstra, A.L.P. Houseman, G.L. Colpas, J.W. Kampf, R. LoBrutto, W.D. Frasch, V.L. Pecoraro. *Inorg. Chem.*, **36**, 4866 (1997).
[14] A. Butler, J.W. Walker. *Chem. Rev.*, **93**, 1937 (1993).
[15] P. Caravan, L. Gelmini, N. Glover, G.F. Herring, H. Li, J.H. McNeil, S.J. Rettig, I.A. Setyawati, E. Shuter, Y. Sun, A.S. Tracey, V.G. Yuen, C. Orvig. *J. Am. Chem. Soc.*, **117**, 12759 (1995).
[16] L.C. Cantley, P. Aisen. *J. Biol. Chem.*, **254**, 1781 (1979).
[17] J.C. Chang, J.A. Labinger, H.B. Gray. *Inorg. Chem.*, **36**, 5927 (1997).
[18] C. Bolm, F. Bienewald. *Angew. Chem. Int. Ed. Engl.*, **34**, 2640 (1995).
[19] K. Nakajima, M. Kojima, K. Toriumi, K. Saito, J. Fujita. *Bull. Chem. Soc. Jpn.*, **62**, 760 (1989).
[20] M. Bagherzadeh, M.M. Haghdoost, A. Shahbazirad. *J. Coord. Chem.*, **65**, 591 (2012).
[21] D.A. Cogan, G. Liu, K. Kim, B. Backes, J.A. Ellman. *J. Am. Chem. Soc.*, **120**, 8011 (1998).
[22] C. Bolm, F. Bienewald. *Synlett*, **34**, 1327 (1998).
[23] D. Rehder. *J. Inorg. Biochem.*, **80**, 133 (2000).
[24] T. Hirao. *J. Inorg. Biochem.*, **80**, 27 (2000).
[25] K. Sato, M. Chikira, Y. Fuji, A. Kamatsu. *J. Chem. Soc. Chem. Commun.*, **5**, 625 (1994).
[26] J. Chang, E. Day Shannon, W.C. Silvers. *J. Electroanal. Chem.*, **622**, 15 (2008).
[27] A. Pui, C. Dobrota, J.-P. Mahy. *J. Coord. Chem.*, **60**, 581 (2007).
[28] H. Shimakoshi, W. Ninomiya, Y. Hisaeda. *J. Chem. Soc., Dalton Trans.*, **13**, 1971 (2001).
[29] L. Xu, Y.Y. Yang, Y.Q. Wang, J.Z. Gao. *Anal. Chim. Acta*, **653**, 217 (2009).
[30] M.F.S. Teixeira, E.R. Dockal, E.T.G. Cavalheiro. *Sens. Actuators, B*, **106**, 619 (2005).
[31] M. Sukwattanasinitt, A. Nantalaksakul, A. Potisatityuenyong, T. Tuntulani, O. Chailapakul, N. Praphairakait. *Chem. Mater.*, **15**, 4337 (2003).
[32] Z.H. Liu, F.C. Anson. *Inorg. Chem.*, **39**, 274 (2000).
[33] P. Adao, M.R. Maurya, U. Kumar, F. Avecilla, R.T. Henriques, M.L. Kusnetsov, J.C. Pessoa, I. Correia. *Pure Appl. Chem.*, **81**, 1279 (2009).
[34] C.D. Brondino, R. Calvo, E.J. Baran. *Chem. Phys. Lett.*, **271**, 51 (1997).
[35] E.J. Baran, P.A.M. Williams, R.S. Puche, J. Soria. *Polyhedron*, **9**, 1383 (1990).
[36] İ. Ucar, E. Bozkurt, C. Kazak, A. Bulut. *Spectrochim. Acta Part A Mol. Biomol. Spectrosc.*, **72**, 11 (2009).
[37] E. Bozkurt, İ. Ucar, I. Kartal, B. Karabulut, Y. Bekdemir. *Z. Kristallogr.*, **224**, 163 (2009).
[38] W.J. Geary. *Coord. Chem. Rev.*, **7**, 81 (1971).
[39] K.S. Patel, G.A. Kolawole. *J. Coord. Chem.*, **11**, 231 (1982).
[40] K.P. Callahan, P.J. Durand. *Inorg. Chem.*, **19**, 3211 (1980).

[41] H. Keypour, M. Shayesteh, R. Golbedaghi, A. Chehregani, A.G. Blacman. *J. Coord. Chem.*, **65**, 1004 (2012).
[42] A. Ghaffari, M. Behzad, G. Dutkiewicz, M. Kubicki, M. Salehi. *J. Coord. Chem.*, **65**, 840 (2012).
[43] M. Kandaz, İ. Yılmaz, S. Keskin, A. Koca. *Polyhedron*, **21**, 825 (2002).
[44] M. Kandaz, A. Koca, A.R. Özkaya. *Polyhedron*, **23**, 1987 (1996).
[45] M. Kato, K. Nakajima, Y. Yoshikawa, M. Hirotsu, M. Kojima. *Inorg. Chim. Acta*, **311**, 69 (2000).
[46] K. Yamamoto, K. Oyaizu, E. Tsuchida. *J. Am. Chem. Soc.*, **118**, 12665 (1996).
[47] R. Ando, S. Mori, M. Hayashi, T. Yagyu, M. Maeda. *Inorg. Chim. Acta*, **357**, 1177 (2004).
[48] P. Plitt, H. Pritzkow, T. Oeser, R. Kraemer. *J. Inorg. Biochem.*, **99**, 1230 (2005).
[49] I. Yilmaz. *Transition Met. Chem.*, **33**, 259 (2008).
[50] E. Tas, I.H. Onal, I. Yilmaz, A. Kilic, M. Durgun. *J. Mol. Struct.*, **927**, 69 (2009).
[51] E. Tas, A. Kilic, M. Durgun, L. Kupecik, I. Yilmaz, S. Arslan. *Spectrochim. Acta Part A Mol. Biomol. Spectrosc.*, **75**, 811 (2010).
[52] U.L. Kala. *Polyhedron*, **26**, 1427 (2007).
[53] B.J. Hathaway, A.A.G. Tomlinson. *Coord. Chem. Rev.*, **5**, 1 (1970).
[54] R.K. Ray, G.B. Kaufman. *Inorg. Chim. Acta*, **153**, 207 (1990).
[55] A.H. Maki, B.R. McGarvey. *J. Chem. Phys.*, **29**, 35 (1958).
[56] V.T. Kasumov, F. Köksal. *Spectrochim. Acta Part A Mol. Biomol. Spectrosc.*, **58**, 2199 (2002).
[57] A.H. Maki, B.R. McGarvey. *J. Chem. Phys.*, **29**, 31 (1958).
[58] J.R. Wasson, C. Trapp. *J. Phys. Chem.*, **73**, 3763 (1969).
[59] A.R. Nicolás, C.S. Karina, Â.B.C.M. Maria, S.M. Antonio, C.P.M. Elene. *J. Braz. Chem. Soc.*, **17**, 497 (2006).
[60] O. Cozar, I. Bratu, L. Szabó, I.B. Cozar, V. Chiş, L. David. *J. Mol. Struct.*, **993**, 397 (2011).
[61] İ. Uçar, B. Karabulut, A. Bulut, O. Büyükgüngör. *J. Mol. Struct.*, **834–836**, 336 (2007).
[62] B. Macias, M.V. Villa, I. Garcia, A. Castineiras, J. Borras, R. Cejudo-Marin. *Inorg. Chim. Acta*, **342**, 241 (2003).